Magnetic stabilization and vorticity in submillimeter paramagnetic liquid tubes

J. Michael D. Coey[a,1], Ryoichi Aogaki[b], Fiona Byrne[a], and Plamen Stamenov[a]

[a]School of Physics and Centre for Research on Adaptive Nanostructures and Nanodevices, Trinity College, Dublin 2, Ireland; and [b]Department of Product Design, Polytechnic University, Sagamihara, Kanagawa 229-1196, Japan

This contribution is part of the special series of Inaugural Articles by members of the National Academy of Sciences elected in 2005.

Contributed by J. Michael D. Coey, March 18, 2009 (sent for review January 21, 2009)

It is possible to suppress convection and dispersion of a paramagnetic liquid by means of a magnetic field. A tube of paramagnetic liquid can be stabilized in water along a ferromagnetic track in a vertical magnetic field, but not in a horizontal field. Conversely, an "antitube" of water can be stabilized in a paramagnetic liquid along the same track in a transverse horizontal field, but not in a vertical field. The stability arises from the interaction of the induced moment in the solution with the magnetic field gradient in the vicinity of the track. The magnetic force causes the tube of paramagnetic liquid to behave as if it were encased by an elastic membrane whose cross-section is modified by gravitational forces and Maxwell stress. Convection from the tube to its surroundings is inhibited, but not diffusion. Liquid motion within the paramagnetic tube, however, exhibits vorticity in tubes of diameter 1 mm or less—conditions where classical pipe flow would be perfectly streamline, and mixing extremely slow. The liquid tube is found to slide along the track almost without friction. Paramagnetic liquid tubes and antitubes offer appealing new prospects for mass transport, microfluidics, and electrodeposition.

fluid dynamics | magnetism | Maxwell stress | microfluidics

Mass transport in miscible liquids is usually dominated by convection. When a drop of colored solution falls into a glass of water, it quickly disperses because of convection driven by density differences and the initial velocity distribution. The relevant dimensionless quantity is the Péclet number Pe, the ratio of the time scales for diffusion and dispersion. This number, defined as

$$\mathrm{Pe} = lv_\mathrm{d}/D, \qquad [1]$$

where D is the diffusion constant, l is a characteristic dimension of the system, and v is the liquid velocity, is usually much greater than 1. A typical value of D for ions in solution is 10^{-9} m^2·s^{-1} (1); the dimension l of our glass is ~0.1 m and v_d may be ~1 mm·s^{-1}, so Pe ~ 10^5. The drop of ink disperses in the glass of water in less than a minute, but to achieve mixing by diffusion would take a time of order $l^2/\pi^2 D$ (1), which is about a fortnight.

A magnetic field can suppress convection in the following way: Magnetization is induced in a paramagnetic liquid by an external field, and a magnetic field *gradient* is created by means of ferromagnetic material to exert a force on the induced magnetization. With an appropriate field configuration, it is possible to confine the paramagnetic liquid in a stable shape. The field gradient force density on an element with uniform magnetization $\boldsymbol{M}$ in an external field $\boldsymbol{H}_0$ is

$$\boldsymbol{F}_\mathrm{m} = \mu_0 \nabla(\boldsymbol{M}\cdot\boldsymbol{H}_0). \qquad [2]$$

A more general expression, valid when the specific magnetization is independent of density, as it is for dilute solutions, is (2, 3):

$$\boldsymbol{F}_\mathrm{m} = \mu_0(\boldsymbol{M}\cdot\nabla)\boldsymbol{H}. \qquad [3]$$

Here $\boldsymbol{H}$ is the local field, which is the applied field corrected for demagnetizing effects. The two expressions are equivalent provided that demagnetizing effects are negligible and $\nabla \times \boldsymbol{H} = 0$, which is true in the absence of electric currents (4, 5). An experimental analysis of magnetic forces in liquids is given in ref. 6.

Confinement, manipulation, and mixing of current-carrying conducting species in microfluidic channels by means of the Lorentz force $\boldsymbol{F}_\mathrm{L} = \mu_0 \boldsymbol{j} \times \boldsymbol{H}_0$, were $\boldsymbol{j}$ is the current density, has been quite thoroughly investigated in electrochemical cells (7–10). Confinement by the magnetic field gradient force is well known in ferrofluids (3), and it has been observed in electrolytes where a reduced paramagnetic species may be trapped in the vicinity of an iron microelectrode (11) or a magnetic nanowire array (12). There are some recent accounts of confinement of paramagnetic solutions in a magnetically-defined channel in microfluidic chip structures (13, 14). Here we explore some remarkable consequences of paramagnetic liquid confinement by the field gradient force, and we analyze the phenomenon quantitatively.

It is important that the two liquids that are to be prevented from intermixing have magnetic susceptibilities that are as different as can be. If one is water, which is weakly diamagnetic with molar susceptibility $\chi_\mathrm{mol} = -0.16 \times 10^{-9}$ m^3·mol^{-1} (dimensionless susceptibility $\chi = -9 \times 10^{-6}$), the other should be a solution containing paramagnetic 3d or 4f ions, or paramagnetic molecular species. The molar susceptibility of a paramagnetic species with angular momentum quantum number J at temperature T is given by the Curie law (5)

$$\chi_\mathrm{mol} = \mu_0 N_\mathrm{A} g^2 \mu_\mathrm{B}^2 J(J+1)/3k_\mathrm{B}T, \qquad [4]$$

where N_A is Avogadro's number, g is the Landé g-factor, μ_B is the Bohr magneton, and k_B is Boltzmann's constant. The formula can be written more simply as $\chi_\mathrm{mol} = \mathrm{C}/T$, where the molar Curie constant is

$$\mathrm{C} = 1.57 \times 10^{-6} p_\mathrm{eff}^2, \qquad [5]$$

and the effective Bohr magneton number is $p_\mathrm{eff} = g[J(J+1)]^{1/2}$. Provided the change of volume of the water caused by the dissolved ions can be neglected, the dimensionless susceptibility of an aqueous solution is

$$\chi = \chi^\mathrm{ions} + \chi^\mathrm{water}, \qquad [6]$$

where $\chi^\mathrm{ions} = c\mathrm{C}/T$ and c is the concentration of the solution in mol·m^{-3}. (A 1 molar solution has c = 1,000 mol·m^{-3}.) Table 1 lists some values of χ_mol and includes the dimensionless susceptibility χ_1M of 1 M aqueous solutions.

Author contributions: J.M.D.C. and R.A. designed research; J.M.D.C. and F.B. performed research; J.M.D.C. and P.S. analyzed data; and J.M.D.C. wrote the paper.

The authors declare no conflict of interest.

Freely available online through the PNAS open access option.

See Profile on page 8808.

[1]To whom correspondence should be addressed. E-mail: jcoey@tcd.ie.

Table 1. Susceptibility of some paramagnetic ions and molecular solutions at 300 K

Ion	Orbital	J	p_{eff}^2	χ_{mol}, $\text{m}^3\cdot\text{mol}^{-1}$	$\chi_{1\text{M}}$
Cu^{2+}	$3d^9$	1/2	3*	16×10^{-9}	7×10^{-6}
Free radicals, NO	$ns^{1,2p}$	"	"	"	"
Ni^{2+}	$3d^8$	1	8*	42×10^{-9}	33×10^{-6}
O_2	2p	"	"	"	"
Co^{2+}	$3d^7$	3/2	15*	79×10^{-9}	70×10^{-6}
Mn^{2+}	$3d^5$	5/2	35*	183×10^{-9}	174×10^{-6}
Gd^{3+}	$4f^7$	7/2	63*	330×10^{-9}	321×10^{-6}
Ho^{3+}	$4f^{10}$	8	112.5	589×10^{-9}	580×10^{-6}
Er^{3+}	$4f^{11}$	15/2	91.8	481×10^{-9}	472×10^{-6}

*$J = S$, $g = 2$.

It is evident from Table 1 that the susceptibility of even the most concentrated solution of paramagnetic ions is much less than unity. As a result, the demagnetizing field $\boldsymbol{H}_{\text{d}}$, which is always less than $\chi\boldsymbol{H}_0$, can normally be neglected. The local field in Eq. **3**, $\boldsymbol{H} = \boldsymbol{H}_0 + \boldsymbol{H}_{\text{d}}$, can be taken to be the same as the applied field, which greatly simplifies analysis of the phenomenon. Specifically, no appreciable force density exists for an inhomogeneous concentration c of paramagnetic solution in a uniform applied field (15). This is readily seen in the Coulomb representation, where a nonuniformly magnetized material is represented by a volume distribution of "magnetic charge" $\rho_{\text{m}} = -\nabla\cdot\boldsymbol{M}$. By definition, $\boldsymbol{B} = \mu_0(\boldsymbol{H} + \boldsymbol{M})$ and $\nabla\cdot\boldsymbol{B} = 0$ (Maxwell's equation). Hence $\rho_{\text{m}} = \nabla\cdot\boldsymbol{H}$, but $\boldsymbol{H} \approx \boldsymbol{H}_0$, which is uniform, so $\rho_{\text{m}} = 0$. This argument does not apply to ferromagnetic colloids such as ferrofluids, where the susceptibility, $\chi \sim 10^{-1}$–10^{-2}, is several orders of magnitude greater than that of the paramagnetic solutions (3). Moreover, we will see that there are observable consequences of very small demagnetizing effects on paramagnetic liquid tubes.

A further simplification arising from the small susceptibility of paramagnetic solutions is that their permeability $\mu = \mu_0(1 + \chi)$ is effectively equal to μ_0, the permeability of free space ($4\pi \times 10^{-7}$ $\text{T}\cdot\text{m}\cdot\text{A}^{-1}$). Their conductivity σ is of order 10 $\Omega^{-1}\cdot\text{m}^{-1}$, so the magnetohydrodynamic diffusivity $\lambda = 1/\sigma\mu \approx 10^5$ $\text{m}^2\cdot\text{s}^{-1}$. The magnetic Reynolds number $\text{R}_{\text{m}} = lv_{\text{d}}/\lambda$ is very small, $\sim 10^{-9}$, which means that motion of the fluid has no influence on the magnetic field. Magnetohydrodynamics in a beaker, unlike magnetohydrodynamics in the Earth's core or in interstellar space, reduces to hydrodynamics + magnetostatics.

An up-to-date account of laboratory-scale magnetic field effects on materials, including magnetoelectrochemistry, levitation, and control of liquid metals can be found in ref. 16.

Experimental Results

We have used 2 M solutions of $NiSO_4$, 1.5 M solutions of $CoCl_2$, and 1 M solutions of $ErCl_3$. The first is green with dimensionless susceptibility $\chi = 75 \times 10^{-6}$, the second is bright red with $\chi = 110 \times 10^{-6}$, and the third is pink with $\chi = 472 \times 10^{-6}$. Water has susceptibility $\chi = -9 \times 10^{-6}$. The visibility of the cobalt solution is best in the experiments we describe.

Form. Various magnetic tracks were prepared by embedding iron wire in molded Lucite plates 30 mm in diameter, in such a way that the wire lies just below the surface of the plastic. Included were straight tracks made of wire of different diameters, ranging from 125 μm up to 1 mm, as well as circular, meandering, X, Y, and $\propto$-shaped tracks. Some were nonuniform in width, others were bifurcated. The plate is immersed in a 50-ml vessel of water and a uniform external magnetic field $\boldsymbol{H}_{\text{a}}$ is applied, using either an electromagnet or a permanent magnet structure. Free-standing iron tracks, completely immersed in liquid, were also investigated. The different magnetic fields and magnetizations involved in the experiments are summarized in Fig. 1.

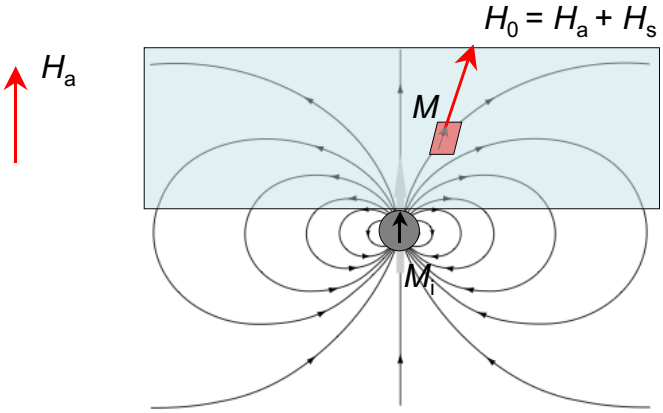

Fig. 1. The different magnetic fields and magnetizations involved in the experiments. M is the magnetization of an element of liquid, M_{i} is the magnetization of the iron track, $\boldsymbol{H}_{\text{a}}$ is the uniform field applied by using a permanent magnet or an electromagnet, $\boldsymbol{H}_{\text{s}}$ is the stray field created by M_{i}, and $\boldsymbol{H}_0 = \boldsymbol{H}_{\text{a}} + \boldsymbol{H}_{\text{s}}$ is the magnetic field acting on M. The demagnetizing field $\boldsymbol{H}_{\text{d}}$ is very small in M, but not in M_{i}.

When a vertical magnetic field of 0.5 T is applied, and paramagnetic solution is carefully injected with a syringe into the water at the end of the track. The solution does not disperse in the water, but forms a colored tube that faithfully follows the track, as illustrated in Fig. 2. Provided the susceptibility and applied field are sufficiently great, the paramagnetic liquid tube has a roughly circular, balloon-like cross-section, just touching the embedded iron track. The injected solution courses rapidly along the track, but it is confined in the perpendicular directions. On continued injection, the paramagnetic liquid tube swells to several times the track diameter, and the bloated tube eventually begins to leak. When the injection is arrested, the tube repairs itself. The paramagnetic liquid seems to behave as if it were encased in a "self-healing" elastic membrane. It is a tube that cannot clog.

Normal diffusion of ions from the tube is *not* suppressed. Tubes were injected along straight tracks of diameters ranging from 125 μm to 1 mm, and the time for the colored solution to diffuse away was measured. Times for $CoCl_2$ and $NiSO_4$ increased from a few seconds for the smallest diameter, up to more than 1,000 s for the largest. Times for $ErCl_3$ were about twice as long. Diffusion constants D were estimated by plotting the diffusion time t_{diff}, subjectively estimated as the time taken for the tube to disappear, against the radius r_{i} of the iron wire. As, in two dimensions, the probability of finding a diffusing ion at a distance r from its initial position is given by $p(r, t) = r^2(Dt)^{-1}$, the time taken to lose visual contrast, corresponding to a reduction of the initial concentration by a certain ratio α, would be given by $t \sim \alpha^{-1}r_0^2D^{-1}$, where r_0 is the initial radius of the liquid tube. The square of the maximal initial tube radius r_0, which is proportional to the volume of the tube, is approximately linearly proportional to the radius of the ferromagnetic wire r_{i} because the magnetic field gradient created is inversely proportional to r_{i}, thus resulting in a relation of the form $t_{\text{diff}} \sim ar_{\text{i}}D^{-1}$, where a is a constant with dimensions of length. It was determined by comparison with numerical calculations based on the diffusion equation, as the product of $(\alpha a)^{-1}$ in decibels per meter is a characteristic of the observer's vision. A value of 0.2 was obtained from visual simulations based on the numerical calculations, which was then used for the determination of D from the data in Fig. 3. Values extracted for the diffusion constants are:

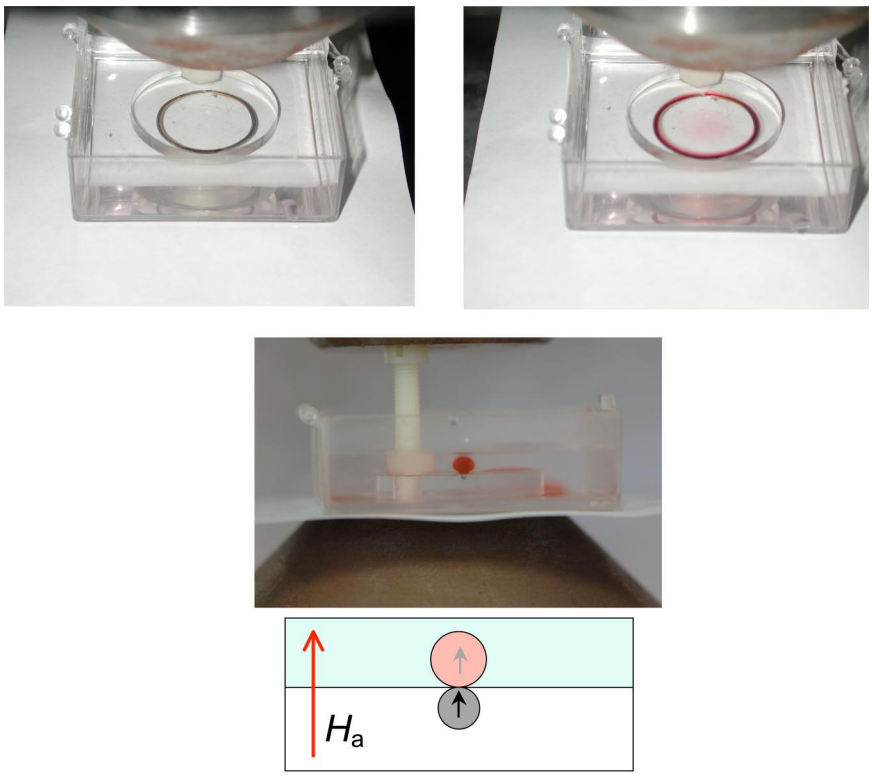

Fig. 2. Formation and cross section of paramagnetic liquid tubes. A circular iron track embedded in a Lucite disc, immersed in water and placed in a vertical magnetic field of 0.5 T (*Upper Left*). When a 1.5 M $CoCl_2$ solution is injected near the track it does not disperse, but forms a paramagnetic liquid tube along the track (*Upper Right*). (*Lower*) The cross-section of a straight tube of 1 M $ErCl_3$ in a vertical field of 1 T.

0.6×10^{-9} $m^2 \cdot s^{-1}$, 0.5×10^{-9} $m^2 \cdot s^{-1}$, and 0.3×10^{-9} $m^2 \cdot s^{-1}$ for $CoCl_2$, $NiSO_4$, and $ErCl_3$, respectively. These are reasonable values for diffusion in ionic solutions (1).

No stabilization is observed in the absence of a ferromagnetic track. Nor is the paramagnetic liquid tube stable when the applied field is horizontal, rather than vertical. All this can be easily understood from the diagrams in Fig. 4. The field gradient force is attractive in the head-to-tail configuration of Fig. 4*A*, where the field is vertical, but it is repulsive in the broadside configuration of Fig. 4*B*, where the field is horizontal. It is, however, possible to stabilize an "antitube" of diamagnetic water in a bath of paramagnetic solution with a horizontal field (Fig. 4*D*), provided the field is applied perpendicular to the track. A parallel field is ineffective, because there is no stray field from a long straight wire, except at the ends. It is the stray field gradient from the ferromagnetic track that stabilizes the paramagnetic liquid tubes.

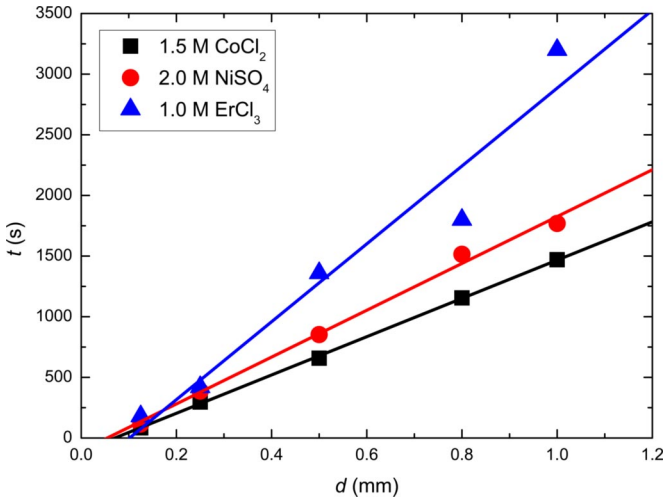

Fig. 3. Time taken for a magnetically-confined paramagnetic liquid tube of 1.5 M $CoCl_2$, 2.0 M $NiSo_4$, and 1.0 M $ErCl_3$ to diffuse away in water, plotted against the diameter of the iron track, $d = 2r_i$.

Another way to stabilize a paramagnetic liquid tube in a horizontal field is to use a double track, where there is a gap between the two parallel iron wires that is comparable to their diameter (13, 15). The paramagnetic tube is stable in water, just above the gap in the double embedded track.

When the iron track is immersed in water, rather than embedded in a plastic base plate, yet more configurations for magnetic confinement are possible. Stable positions for a paramagnetic liquid tube are above and below the wire in a vertical field, and at either side of it in a transverse horizontal field. The converse is true for an antitube. The $ErCl_3$ solution, which has specific gravity 1.1, is shown cradled above the wire in Fig. 5*C*), and suspended beneath it in Fig. 5*B*). With the help of double immersed tracks in a horizontal field, it is possible to direct paramagnetic liquid tubes to any desired point in a vessel of water.

The situation is different when the wire is *permanently* magnetized, and the externally applied field $\boldsymbol{H}_a = 0$. In that case, $\boldsymbol{M}$ is nonuniform and both the magnetizing field $\boldsymbol{H}_0$ and the field gradient are due to the wire. The paramagnetic liquid tends to gather around the wire in the form of a sheath, but then falls away, under the influence of gravity.

Flow. The average flow velocity v in normal laminar pipe flow, where there is a no-slip boundary condition at the pipe wall, is given by Poiseuille's equation $v = r_p^2 \Delta P / 8\eta l$ (17). Here $\Delta P/l$ is the pressure gradient, r_p is the pipe radius, and η is the viscosity of

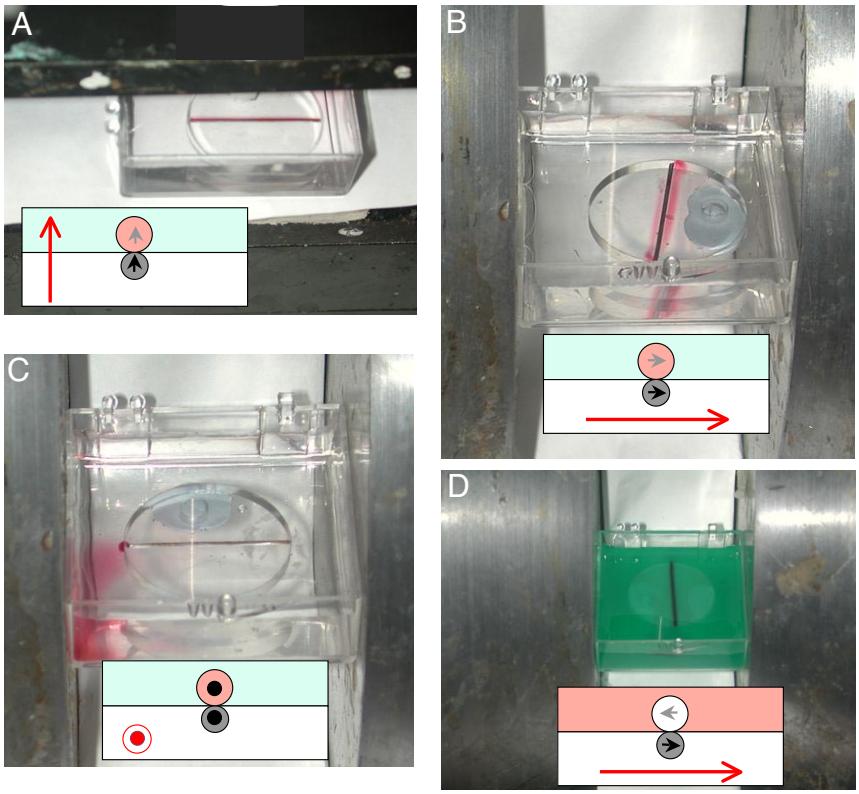

Fig. 4. Stable and unstable configurations for paramagnetic liquid tubes. Configurations where magnetic confinement of a liquid can be achieved are a tube in a vertical field (*A*) and an antitube in a horizontal field (*D*). The water is dyed black in *D* for visibility. The paramagnetic liquid is colored pink in the diagrams, and the water pale blue. The magnetization of the iron wire is indicated by the black arrow, and that of the paramagnetic liquid by the gray arrow. The water in *D* has an effective moment indicated by the gray arrow. Dipole forces are attractive in *A* and *D* but repulsive in *B* and *C*.

the liquid (1 mN·m^{-2}·s for water). Large pressure gradients are needed to generate modest flows in small tubes. The flow rate is $\pi r_p^2 v$, which varies as r_p^4. Flow is determined by the no-slip boundary condition at the wall of the pipe, which leads to a parabolic velocity profile across the diameter.

The nature of the fluid flow in the paramagnetic liquid tube is remarkably different; it is scarcely more difficult to inject the liquid along the magnetic track in a vessel of water than it is to eject the liquid from a syringe. The flow is almost frictionless (13), because movement of the paramagnetic liquid tube entrains movement of the surrounding water. When some ink was introduced into the water, the ink was seen to be dragged along with the liquid in the moving tube. Except at the surface of the track, the liquid at the boundary of the tube is moving, not stationary as in pipe flow. The effective radius r_{eff} is many times the actual radius r_p of the paramagnetic liquid tube, and the pressure gradient is reduced and the flow rate is increased accordingly. The roughly circular cross-section of the static tube is observed to change, becoming squarer as it begins to move.

The absence of a stationary containing wall means that there is little radial velocity stratification in the tube. Normally laminar (streamline) flow is found in pipes with diameters of a millimeter or less because Reynolds number $\text{Re} = 2v\rho r_p/\eta$ is of order 1–10, for typical velocities of a few millimeters per second. Turbulence in pipes sets in only when Re exceeds 2,000 (12). The nature of the flow in a paramagnetic liquid tube is contrasted with that in a pipe in Fig. 6. When two streams of liquid, colored red and green, are injected into a closed Y-shaped channel with rectangular cross-section in the transparent plastic they do not mix, but flow along in parallel. Streamline flow is the bane of microfluidics, where an aim is often to get the contents of a narrow channel to mix as soon and as thoroughly as possible. Mixing liquids at the microliter (cubic millimeter) level is "like trying to stir molasses into honey" (18). The length of channel necessary for mixing is $2r\text{Pe}$, which is many meters. Various mixing strategies have been proposed to get around the problem [refs. 19–23; ref. 23 and the 10 following papers (*Philos Trans R Soc London A* 362:923–1129) provide a recent overview of mixing at the microscale].

Flow in the paramagnetic liquid tube is quite different, as seen in Fig. 6 *Lower*. When two streams of paramagnetic liquid, differentiated by their color, are injected along either arm of a Y-shaped ferromagnetic track, they mix almost as soon as they meet. Dispersion is not suppressed *within* the tube because there are no strong velocity gradients there. It is impeded only at the interface between the confined magnetic tube and the water. Flow in paramagnetic liquid tubes with radii as small as 100 μm gives the impression of being turbulent. Vortices form close to where the two liquids are injected at flow velocities as low as $v \approx 1$ mm·s^{-1}.

Discussion

The reason for the stabilization of the paramagnetic liquid tube by the iron track is the interaction of the stray field gradient ∇H_s with the magnetization $\boldsymbol{M} = \chi \boldsymbol{H}$ that is induced in the paramagnet by the total magnetic field $\boldsymbol{H}_0$ acting upon it (3). The force density at a point in the magnetized liquid is deduced from Eq. **2**; in polar coordinates

$$F_r = \mu_0[M_r(\partial H_r/\partial r) + M_\theta(\partial H_\theta/\partial r)]$$
$$F_0 = \mu_0[M_r(1/r)(\partial H_r/\partial \theta) + M_\theta(1/r)(\partial H_\theta/\partial \theta)]. \quad [7]$$

The magnitude of this force density F is $\sim \mu_0 H_0 \Delta\chi |\nabla H|$. Here $\Delta\chi$ is the difference in dimensionless susceptibility between the paramagnetic solution and the water, and H is the field, in A·m^{-1}

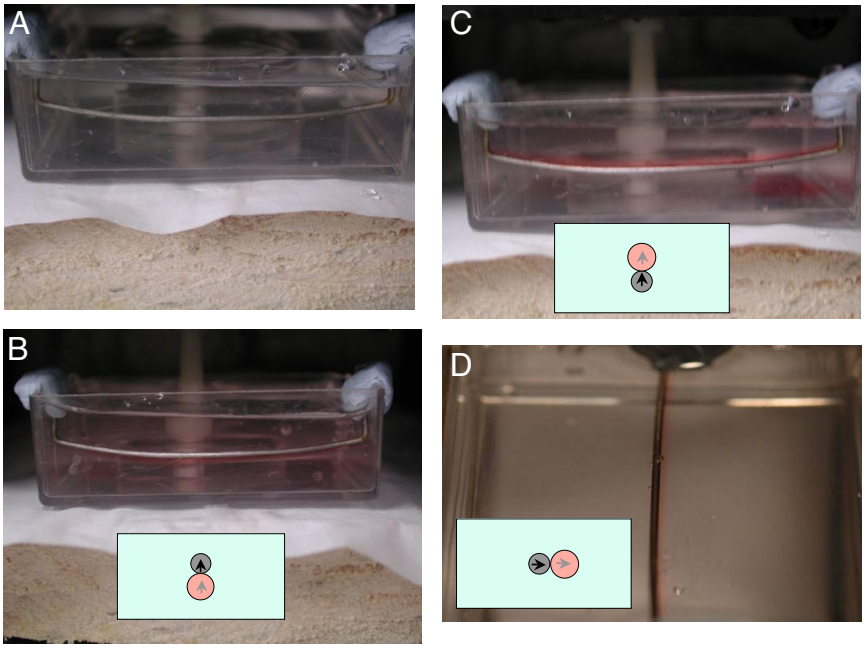

Fig. 5. Paramagnetic liquid tubes stabilized by an immersed track. (*A*) An iron wire immersed in water. (*B–D*) Stable positions for a paramagnetic liquid tube are above (*C*) and below (*B*) the ferromagnetic wire in a vertical field, and at either side of it in a horizontal field (*D*). The photographs show tubes of $ErCl_3$ in water.

acting at any point. In our experiments $\mu_0 H_a \approx 0.5$ T, $\Delta\chi \approx 100 \times 10^{-6}$, $\nabla H_0 \approx M_i/(r_i^2/r^3) \approx 10^9$ A·m^{-2}, where $M_i \approx 1$ MA·m^{-1} is the magnetization of iron and $r \approx r_t \approx 1$ mm. Hence $F \approx 10^5$ N·m^{-3}, which exceeds the force density due to gravity $F_g = \rho g$. Field gradient forces really are of this magnitude, as is easily seen by placing a beaker of paramagnetic solution in the fringing field of an electromagnet and observing the deformation of the liquid surface. The density differences driving convection are of order 100 kg·m^{-3}, so the magnetic field gradient force can easily overcome the resulting buoyancy forces. Furthermore, liquid with an initial dispersive velocity of $v_d = 1$ mm·s^{-1} can only drift a distance $v_d^2\rho/2F$, or much less than 1 μm in the gradient field.

The confinement of the paramagnetic liquid tube and the elastic-membrane-like quality of the interface between it and the surrounding water are essentially attributable to the magnetic field gradient force, Eq. **2**. The contribution from the difference in surface tension between water and an ionic solution, which increases proportionally to the ionic strength for concentrated solutions (24), is only about $2M'$ mN·m^{-1} (25), where M' is the molarity of the solution. This is small compared with the surface tension of water in air (72 mN·m^{-1}), and the corresponding force density for a 1-mm tube is of order 10^3 N·m^{-3}. We first calculate the influence of the main stabilizing factor, the magnetic field gradient force density on the shape of the tube in two limiting cases, and then we consider factors that tend to deform the shape of the tube, namely gravity and Maxwell stress

(*i*) $H_a = 0$: Here $\boldsymbol{H}_0 = \boldsymbol{H}_s$, $\boldsymbol{M} = \chi \boldsymbol{H}_s$. The stray field in polar coordinates $\boldsymbol{H}_s = [H_r, H_\theta]$ due to a long straight wire of radius r_i with a transverse permanent magnetization M_i is

$$\boldsymbol{H}_s = (M_i r_i^2/2r^2)[\cos\theta, \sin\theta]. \quad [8]$$

The magnitude of the stray field depends only on the radial coordinate r, not on the angular coordinate θ. Because $\boldsymbol{M} = \chi \boldsymbol{H}_s$, the force is in the inward radial direction, as can be verified by substitution in Eq. **2**. The contour of the paramagnetic liquid tube in this case is circular and concentric with the wire. The surface of the tube can be regarded as a contour of constant energy gradient $(1/2)\mu_0\chi H_s^2$, r = constant.

(*ii*) $H_a \gg H_s$: Here $\boldsymbol{M} \approx \chi \boldsymbol{H}_a$, $\nabla H_0 = \nabla H_s$. The magnetization of the liquid is in the direction of the applied field, assumed to be vertical. The magnetization is then

$$\boldsymbol{M}\chi H_a[\cos\theta, -\sin\theta]. \quad [9]$$

A magnetization M_0 is induced in the track by the transverse field; the demagnetizing factor of the circular wire is 0.5, so the magnetization induced in the iron wire by the applied field $\mu_0 H_a = 0.5$ T is $\mu_0 M_i = 1.0$ T. From Eqs. **8** and **9** the energy density of the magnetized liquid in the inhomogeneous stray field of the iron track is

$$\mu_0 M H_s = \mu_0 \chi H_a M_i (r_i^2/2r^2)\cos 2\theta. \quad [10]$$

When the track has a radius that is small compared with the height h of the tube, the force density exerted on the paramagnetic liquid by the track, deduced from Eq. **2** or **3**, is

$$\boldsymbol{F} = -\mu_0 \chi H_a M_i (r_i^2/r^3)[\cos 2\theta, \sin 2\theta]. \quad [11]$$

The origin is taken at the center of the track. The force is attractive when $-\pi/4 < \theta < \pi/4$ or $3\pi/4 < \theta < 5\pi/4$, but repulsive otherwise. The surface of the paramagnetic liquid tube must be normal to $\boldsymbol{F}$, with a tangent at a point (r, θ) in a direction $[-\tan 2\theta, 1]$. The contour of the tube obtained by integration is

$$r = h(\cos 2\theta)^{1/2}. \quad [12]$$

The observed cross-section of the tube in Fig. 2 *Lower*, shown enlarged in Fig. 7 *Upper Left*, is essentially of this balloon-like form. The form of the tube in the general case can be solved numerically by calculating the contour of constant energy gradient. The condition $H_a \gg H_s$ is relaxed, and nonuniformity of the magnetization of the liquid close to the iron wire can be taken into account. The results in Fig. 7 *Lower* resemble the profile given by Eq. **12**.

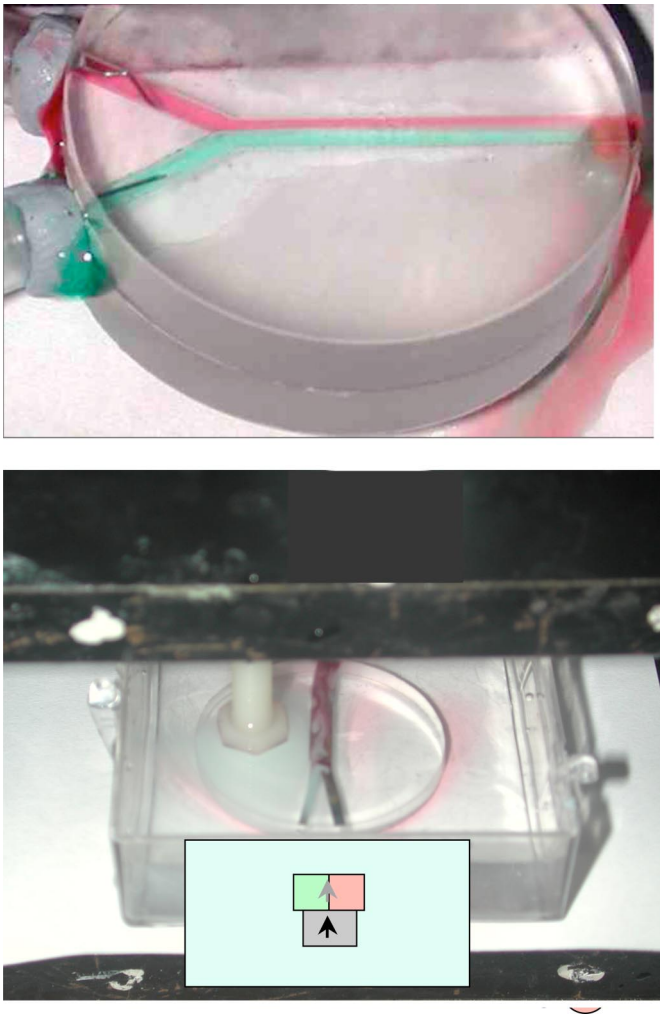

Fig. 6. Comparison of streamline flow of two paramagnetic liquids colored red and green in a transparent rectangular channel (*Upper*) and vortex flow (*Lower*) in a paramagnetic liquid tube with the same dimensions.

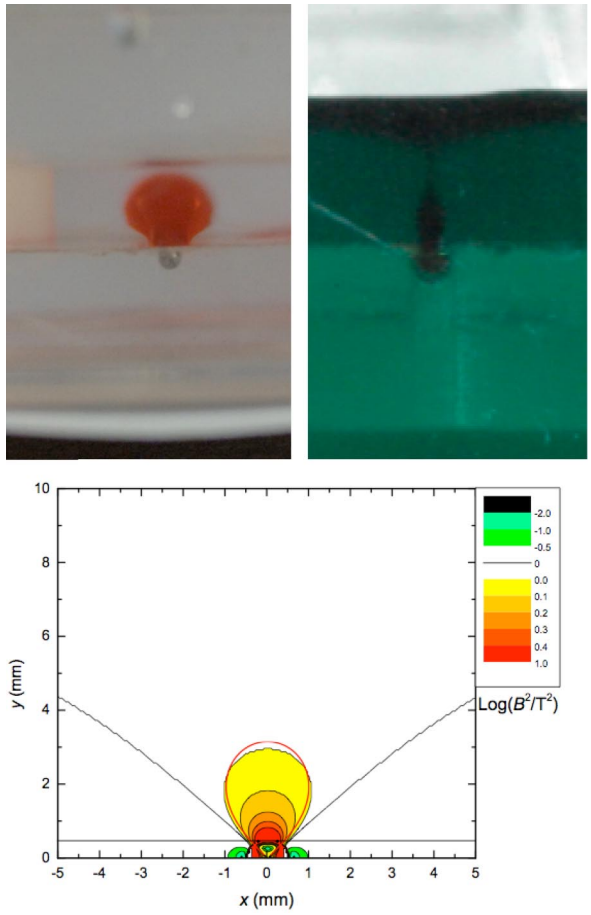

Fig. 7. Observed and calculated cross-sections. Cross-sections of a paramagnetic liquid tube (*Upper Left*), and an antitube (*Upper Right*). In *Upper Left* the Maxwell stress and gravitational deformations tend to cancel, whereas in *Upper Right* they add. (*Lower*) Constant energy surfaces for a 0.5-mm iron wire calculated numerically; the profile corresponding to the analytical approximation of Eq. **12** is indicated by the red line.

The basic shape determined by the magnetic field gradient will be deformed by the two factors mentioned earlier, gravity and Maxwell stress, f_M (2). Density differences between the tube and the surrounding medium tend to make the cross-section more oblate or more prolate depending on whether the tube or the surroundings is the denser. Maxwell stress favors an elongated, prolate cross-section in a vertical field.

The Maxwell stress is most easily understood in the Coulomb representation. Besides the bulk charge density related to nonuniform magnetization $\rho_m = -\nabla\cdot\boldsymbol{M}$ mentioned in Introduction, there is also a surface charge density $\sigma_m = \boldsymbol{M}\cdot\mathbf{e}_n$, where $\mathbf{e}_n$ is a

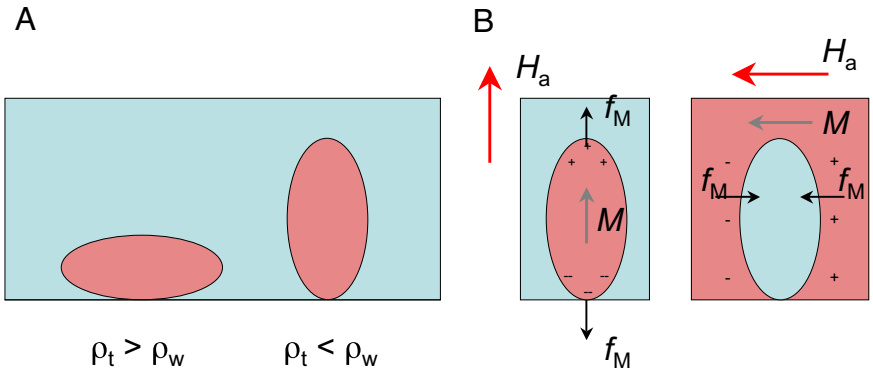

Fig. 8. Schematic illustration of the deformations of a liquid tube due to density differences (*A*), and Maxwell stress on a paramagnetic liquid tube (*B Left*) and on an antitube (*B Right*).

unit vector normal to the surface of the magnetized body. There is therefore a *stress* of magnetic origin on a magnetized body in a uniform field, as shown in Fig. 8. Basically, this "stress" is a demagnetizing effect. The surface charge produces the demagnetizing field, which is reduced by elongating the sample, and thus is an equivalent, but more convenient, representation of the problem of total energy minimization upon volume conservation in external magnetic field. Shape changes are possible in the liquid state, even though σ_m is really small. The stress makes no contribution to the stability of the paramagnetic liquid tube; indeed, it tends to pull it apart, deforming the shape of the tube when it forms. The influence of Maxwell stress in the solid state is negligible—the stress on a ferromagnet with $M = 1$ MA·m^{-1} in a field of 1 T is 10^6 N·m^{-2}, which produces a strain of only 10 ppm in a solid with an elastic modulus of 100 GPa. However, liquids have no shear modulus, and no fixed shape, so the effect of Maxwell stress can be more dramatic.

The deformations due to gravity and Maxwell stress cancel for a tube of radius $r \approx f_M/\Delta\rho g$. Taking $f_M = (\mu_0/2)MH_0$ for a tube with circular cross-section, and $\mu_0 H_0 = 0.5$ T, this radius is 10 mm in a paramagnetic liquid tube with a density ρ 10% greater than the ambient water and a susceptibility of 100×10^{-6}. Hence the Maxwell stress is more important than gravity for deforming our tubes.

Comparing the magnitude of the field gradient force density $F_m = \mu_0 M \nabla H_0$ with that of the Maxwell stress for a tube of circular cross-section, $F_M = \mu_0 H_0 M/\pi r_t$, the ratio is about $\pi r_t/r_i$, or around 10 for the tube shown in Fig. 2 *Upper Right*). The Maxwell stress will have a significant influence on smaller tubes, which will tend to be more prolate.

The situation is different for antitubes. Here all of the factors collude to produce a prolate distortion of the cross-section given by Eq. **12**. The density difference now favors an extension (Fig. 8), and the Maxwell stress in the horizontal field needed to stabilize the antitube squeezes it in the field direction, producing an extension in the direction normal to the substrate. This is all nicely demonstrated by the narrow cross-section of the antitube in Fig. 7 *Upper Right*. When overfilled, the antitube tends to leak along the top edge under the combined influence of Maxwell stress and gravity.

The vortex formation when two streams of paramagnetic liquid are injected onto the same magnetic track (Fig. 6) is not due to turbulence, but to the Kelvin–Helmholtz instability, which is known to create mixing at low Reynolds number (26). When two parallel streams are moving with slightly different velocities, any instability that develops at the interface is amplified by Bernoulli's principle. As it grows, a double spiral vortex develops. The wavelength of the vortices is about seven times the width of the tube (26). This type of vorticity folds the two liquids together on ever-smaller scales, and thereby enables intermixing by diffusion over a length scale that is very much smaller than the radius of the tube.

Conclusion

Thanks to the accessible magnitudes of the magnetic fields required, there may be attractive prospects for applications of paramagnetic liquid tubes, perhaps containing solutions of rare earth ions for maximum susceptibility contrast. Rapid heat exchange by advection can be achieved in small spaces. In biological microfluidics, for example, where channels are typically a few hundred micrometers in diameter, the antitube concept could be useful because the magnetically stabilized tube where rapid mixing occurs is essentially pure water, although even minor amounts of diffusion could lead to toxicity problems. Cytotoxicity of the rare-earth ions merits investigation. Diffusion at the interface can be suppressed by using a solvent for the magnetic ions that is immiscible with water. Turbulent phenomena, which previously were studied on a large scale, in streams, the atmosphere, or in astronomical plasmas, and in laboratory demonstrations (27), can now be examined in controlled conditions on the millimeter scale.

ACKNOWLEDGMENTS. We are grateful to Wiebke Drenckhan and Dennis Weaire for helpful discussions. The work was supported by Science Foundation Ireland, as part of the Magnetic Nanostructures and Spin Electronics project.

1. Cussler EL (1997) *Diffusion, Mass Transfer in Fluid Systems* (Cambridge Univ Press, Cambridge, UK), pp 142–154.
2. Landau LD, Lifschitz EM (1984) *Electrodynamics of Continuous Media* (Pergamon, Oxford), pp 126–128.
3. Rosensweig A (1997) *Ferrohydrodynamics* (Dover, New York), pp 13, 25–31, 110–118.
4. Boyer TH (1988) The force on a magnetic dipole. *Am J Phys* 56:688–691.
5. Coey JMD (2009) *Magnetism and Magnetic Materials* (Cambridge Univ Press, Cambridge, UK), in press
6. Lahoz DG Walker G (1975) An experimental analysis of electromagnetic forces in liquids. *J Phys D* 8:1994–2001.
7. Aogaki R, Fukei K, Mukaibo T (1976) Diffusion process in viscous flow of electrolyte solution in magnetohydrodynamic pump electrodes. *Denki Kagaku* 44: 89–94.
8. Grant KM, Hemmert JW, White HS (2002) Magnetic field-controlled microfluidic transport. *J Am Chem Soc* 124:462–467.
9. Xiang Y, Bau HH (2003) Complex magnetohydrodynamic low-Reynolds-number flows. *Phys Rev E* 68:016312.
10. Arumugam PU, et al. (2006) Redox magnetohydrodynamics in a microfluidic channel. *J Electrochem Soc* 153:E185–E194.
11. Pullins MC, Grant KM, White HS (2001) Microscale confinement of paramagnetic molecules in magnetic field gradients surrounding ferromagnetic microelectrodes. *J Phys Chem B* 105:8989–8994.
12. Chaure N, Coey JMD (2009) Enhanced oxygen reduction at composite electrodes producing a large magnetic gradient. *J Electrochem Soc* 156:F39–F46.
13. Aogaki R, Ito E, Ogata M (2006) Application of magnetic microfluidic chip to chemical and electrochemical reactions. *Magnetohydrodynamics* 42:351–362.
14. Aogaki R, Ito E, Ogata M (2007) A new flow-type cell by the application of magnetic microfluidic chip. *J Solid State Electrochem* 11:757–762.
15. Coey JMD, Rhen FMF, Dunne P, McMurry S (2007) The magnetic concentration gradient force – Is it real? *J Solid State Electrochem* 11:711–717.
16. Yamaguchi M, Tanimoto Y, eds (2006) *Magneto-Science* (Kodansha/Springer).
17. Davidson PA (2004) *Turbulence* (Oxford Univ Press, Oxford), p 10.
18. Knight J (2002) Honey, I shrunk the lab. *Nature* 418:474–475.
19. Bau HH, Zhong J-H, Yi M-Q (2001) A minute magnetohydrodynamic (MHD) stirrer. *Sensors Actuators B* 79:207–215.
20. Lu L-H, Ryu KS, Liu C (2002) A magnetic microstirrer and array for microfluidic mixing. *J Micromech Syst* 11:462–469.
21. Stroock AD, et al. (2002) A chaotic mixer for microchannels. Science 295:647–651.
22. Tabeling P (2003) *Une Introduction à la Microfluidique* (Belin, Paris).
23. Ottino JM, Wiggins S (2004) Introduction; Mixing in microfluidics. *Philos Trans R Soc London A* 362:923–935.
24. Bier M, Zwanikken J, van Roij R (2008) Liquid-liquid interfacial tension of electrolyte solutions. *Phys Rev Lett* 101:046104.
25. Aveyard R, Saleem SM (1976) Interfacial tensions at alkane-aqueous electrolyte interfaces. *J Chem Soc Faraday Trans 1*, 72:1609–1617.
26. Lesieur M (1994) *La Turbulence* (Presses Universitaires de Grenoble), pp 55–67.
27. Thorpe SA (1971) *J Fluid Mech* 46:299–319.